A&A 664, A85 (2022)
https://doi.org/10.1051/0004-6361/202243520

Astronomy & Astrophysics

Methanediol $CH_2(OH)_2$ and hydroxymethyl CH_2OH^+: key organic intermediates on the path to complex organic molecules

Cristopher Heyser Valencia[1] and Natalia Inostroza-Pino[2]

[1] Universidad Autónoma de Chile, Facultad de Ingeniería, Instituto de Ciencias Químicas Aplicadas, Núcleo de Astroquímica & Astrofísica, Av. Alemania 01090, Temuco, Chile
[2] Universidad Autónoma de Chile, Facultad de Ingeniería, Instituto de Ciencias Químicas Aplicadas, Núcleo de Astroquímica & Astrofísica, Av. Pedro de Valdivia 425, Providencia, Santiago, Chile
e-mail: natalia.inostroza@uautonoma.cl

Received 10 March 2022 / Accepted 24 May 2022

ABSTRACT

Context. Ab initio molecular dynamics simulations were carried out to study the formation pathways to complex organic molecules when a OH^+ projectile hit an interstellar dust grain covered only by methanol molecules. The selected target material is a methanol cluster formed by ten units $(CH_3OH)_{10}$.
Aims. The focus of this paper is the process where methanediol $CH_2(OH)_2$ and hydroxymethyl CH_2OH^+, both key organic intermediate molecules, were involved in the formation mechanisms of stable complex organic molecules (COMs).
Methods. We performed Born-Oppenheimer (ab initio) molecular dynamics (BOMD) simulations under the hybrid functional of Head-Gordon ωB97X-D. We used the initial kinetic impact energy of 10, 12, 15, 18, 20, and 22 eV.
Results. We corroborate that $CH_2(OH)_2$ and CH_2OH^+ are the main precursors to form molecules such as methoxymethanol CH_3OCH_2OH, the formyl radical HCO, the Criegee biradical CH_2OO, and formaldehyde H_2Co and its elusive HCOH isomer. We discuss the mechanism formation of these complex organic molecules. We compare the formation pathways with previous theoretical results where both key intermediates are present. The pathways in some cases go through $CH_2(OH)_2$ or undergo by CH_2OH^+.
Conclusions. We confirm that $CH_2(OH)_2$ and CH_2OH^+ play a key role on the path to the formation of abundant H_2CO. These mechanisms can give insight into alternative pathways relevant to understanding experimental processes with key steps within those precursors.

Key words. astrochemistry – molecular processes – ISM: molecules – ISM: abundances – dust, extinction

1. Introduction

To date, more than 200 different molecules have been detected in space, and one of the main questions in astrochemistry is how these molecules are produced. It is widely accepted that interstellar dust grains are covered by frozen molecular species forming a layer known as the ice mantle (Shingledecker et al. 2019), with water ice the dominant component (Öberg et al. 2011), followed by CH_4 and CH_3OH (Hama & Watanabe 2013; Boogert et al. 2015), among other atoms and molecules. Even though water is the most common ice in the interstellar medium (ISM), CH_3OH is a crucial molecule because CH_3OH ice mantles are one of the main proposed sources of complex organic molecules (COMs) (Öberg et al. 2009; Garrod 2008). It has similar volatility to water ice (Brown & Bolina 2007); thus, methanol should reside on grains, as has been confirmed in various ISM studies (Taban et al. 2003; Brown & Bolina 2007). These ices, which are continuously exposed to radiation fields (e.g., UV or X-rays, solar wind particles, or cosmic rays), can produce an interplay between ice chemistries. These interplays yield complex molecules. However, the interplays are still poorly understood. As far as we know, the ice chemistry depends on which atoms or molecules impact the grain and how they stick to its surface; if there is enough thermal energy in the grain, these species may be mobile, allowing them to react using the surface as a catalyst. Finally, if a molecule is to be formed, it must sublimate and be released to the gas phase, where detection occurs. In this context several laboratory experiments (Öberg et al. 2009; Oberg 2016; Yocum et al. 2021; Burke et al. 2015) have been undertaken in order to understand the ice chemistry. One of the relevant reactions in the interstellar medium is precisely the reaction between $CH_3OH + OH^{\bullet}$. This reaction was studied by Oberg (2016), using ices rich in methanol. The authors were able to observe that these ices generated species such as CH_3O, CH_3OCH_3, and CH_2OH. Although they claimed that the identification of the products in the laboratory is a fact, the step-by-step formation mechanisms are not well understood. It is well accepted that the COM formation processes that happen over a grain surface under ISM conditions are not easy, especially when the reaction involves highly unstable species or has not yet been observed experimentally. This has led to the rapidly growing interest in using theoretical tools to study chemical mechanisms and energetics of interstellar reactions difficult to identify and study experimentally, since most of them are reactive radicals. Even when relevant contributions have demonstrated that the energy dissipation is well represented when large icy surfaces are employed (Fredon & Cuppen 2018; Fredon et al. 2017; Pantaleone et al. 2020, 2021), a variety of theoretical approaches must be applied to understand how COMs are formed and released into the gas phase. Thus, theoretical works based on astrochemical modeling (Garrod 2008; Garrod et al. 2007; Kent et al. 2003; Barrientos et al. 2014) have been carried out,

making significant contributions in these fields. For example, research by Yocum et al. (2021) has shown that methanol can form on ice surfaces at low temperatures, confirming an idea that Tielens & Hagen (1982) posited. Works based on quantum chemical simulations have also contributed to previous theoretical investigations on CH_3OH ice mantle impacted by OH projectiles (Inostroza-Pino et al. 2020, 2021) yielding methanediol and hydroxymethyl to produce methoxymethanol CH_3OCH_2OH (McGuire et al. 2017), H_2CO, HCOOH, and OCH_2OH radicals, suggesting that precursor molecules must exist in interstellar ices. This possibility is yet to be investigated. A recent experimental and theoretical quantum investigation points out that simulations with high accuracy using a large ice cluster are very demanding (Miyazaki et al. 2020; Tsuge & Watanabe 2021). Thus, an alternative approach for those calculations was to use small clusters as a realistic amorphous model to interpret the redshift observed under their experiments (Miyazaki et al. 2020). The authors provide insights into the photodesorption of OH radicals, including calculations of binding energies of the OH-ice complex. Additionally, the works by Fredon et al. (2017) and Fredon & Cuppen (2018), for example, demonstrated that desorption depends on the injected kinetic energy and binding energy of the species via classical molecular dynamics (MD) simulations. Furthermore, it is generally agreed that the structure of interstellar dust grains is amorphous upon formation. However, simulations performed by Pantaleone et al. (2020) used a crystalline water-ice surface to show how the energy released by the HCO formation is transferred toward the crystalline water surface. The authors selected this model because tuning the computational setup is easier. In this way, all experimental and theoretical works approximations are needed. Considering that the COM formation in the ISM is still far from being well understood, and many questions on the physics of ISM gas and dust remain open, new theoretical studies based on quantum chemical simulations, as presented here, provide additional information on the COM mechanism formation processes to improve the gas-grain models. We thus selected a cluster model made of ten molecules of methanol to simplify the problem and focus on the reactivity of methanol when receiving an impact of OH-related species, with the goal to analyze pathways that include $CH_2(OH)_2$ and CH_2OH as intermediate molecules. The compound methanediol $CH_2(OH)_2$ is a volatile organic compound (VOC), the simplest elusive diol in organic chemistry, recently synthesized for the first time (Zhu et al. 2022). In an aqueous solution, it is obtained from the hydration reaction of formaldehyde H_2Co. It is an intermediate in the production of aerosols and in reactions that occur in the ozone layer of the atmosphere (ozonolysis), such as the generation of formic acid (HCOOH) (Franco et al. 2021). Processes in the aqueous phase go through $CH_2(OH)_2$ dehydration, and $CH_2(OH)_2$ oxidation in the gas phase. On the other hand, the hydroxymethyl cation CH_2OH^+ is one of the daughter species observed in mass spectra when the C–C–O bonds present in alcohols are broken (Chen et al. 2005).

Consequently, in this work the starting point is the analogue of ice mantles formed by methanol molecules interacting with an energetic OH^+ projectile, mimicking the effects of secondary or tertiary processes in which $CH_2(OH)_2$ and CH_2OH^+ are created to generate COMs. In Sect. 2 we describe the computational methods that were performed, followed by the Sect. 3 on results and discussion. Finally, in the Conclusion we summarize the differences between the theoretical pathways that lead to the formation of different COMs that involve the $CH_2(OH)_2$ and CH_2OH^+ intermediates.

2. Computational methods

We selected a pure ten-unit methanol to mimic a dust cover by a hypothetical molecular mantle formed, in this case, by methanol. This ice mantle represents a small ice region with millions of methanol molecules in only a tiny grain region ($1\,mm^3$). Even though our cluster size is rather limited and the results can be affected by this approach, these simulations allow us to observe whether the newly formed species has enough energy to break its interactions with the methanol mantle and, consequently, to be injected into the gas phase. This allows us to focus on the reactivity of methanol when receiving an impact from OH-related species.

As it is generally agreed that the proper structure of interstellar ice is amorphous upon formation (Maté et al. 2020), we built up a methanol ice mantle model using the cluster amorphous approach (Gadre et al. 2014). Boyd & Boyd (2007) studied clusters of (CH_3OH_n), with $n = 2 \rightarrow 12$ units. They found that ring clusters of n-molecules are more stable than branched-ring and chain clusters, due to the presence of hydrogen bonding (Boyd & Boyd 2007). Furthermore, it was demonstrated that the energetic properties for ring clusters formed by more than six methanol molecules remain approximately constant (Pires & DeTuri 2007). Considering these factors, we selected an optimized ring structure formed by ten units of methanol $(CH_3OH)_{10}$ because its size is an excellent way of reducing computational expense, and also because it is a good representation of a dust ice mantle formed by methanol.

Born-Oppenheimer (ab initio) molecular dynamics (BOMD) simulations were carried out to study the formation pathways where $CH_2(OH)_2$ and CH_2OH are intermediates. With this purpose, we set up a cluster to represent an icy-grain model as a target material. This cluster was hit by an OH^+ projectile mimicking an interstellar dust grain covered only by methanol molecules. Moreover, a comparison of these results was made with the previous process observed after the impact of OH^-, $OH^\bullet$, and OH^+ projectiles (Inostroza et al. 2019; Inostroza-Pino et al. 2020, 2021). Density functional theory calculations under a micro-canonical ensemble (NEV ensemble) were performed with the hybrid functional of Head-Gordon ωB97X-D (Helgaker et al. 1990; Uggerud & Helgaker 1992; Bolton et al. 1998; McBride et al. 2013) and the Pople Basis Set 6-31+g(d,p) (Gordon 1982; Check et al. 2001; Borrás-Almenar et al. 2001). As Inostroza-Pino et al. (2020, 2021), we divided a sphere symmetrically to obtain 24 initial impact positions (Inostroza-Pino et al. 2020). For each hit, the species were in their ground state and the projectile always faced the center of mass of the $(CH_3OH)_{10}$ ice mantle. The initial kinetic impact energies of 10, 12, 15, 18, 20, and 22 eV employed here are the same as those previously used for the OH^-, $OH^\bullet$, and OH^+ projectiles (Inostroza et al. 2019; Inostroza-Pino et al. 2020, 2021).

In the outflows, dust grains generally move with their equilibrium drift velocity up to $\sim 30\,km\,s^{-1}$ corresponding to roughly 20 eV with respect to the gas when the shock is passing (Burkhardt et al. 2019). In addition, the X-rays emitted from the central young stellar object (YSO) can irradiate interstellar ices in the disk, typically generating a span from 0.1 to at least 10 keV (Dupuy et al. 2018). Thus, the ideal conditions for observing similar phenomena to those described here, where the high impact energy is reasonable (Van de Sande et al. 2019), are regions such as asymtotic giant branch (AGB) outflow (Van de Sande et al. 2019). Consequently, we focus only on collisions with initial kinetic energies of 10 eV, 12 eV, 15 eV, 18 eV,

Table 1. Chemical pathways obtained from a $(CH_3OH)_{10}$ ice mantle in collision with a OH^+ projectile with kinetic energy of 10–22 eV.

Reaction N^o	Steps	Products	Impact Energy [eV]
$(CH_3OH)_{10} + OH^+$			
1	1.1	$CH_2(OH)_2 + H^+$ [(a)]	10, 15, 18
2	2.1	$CH_2(OH)_2 + H^+$	
	2.2	$:C(OH)_2 + H_2 + H^+$	20
3	3.1	$CH_3OH \ldots OH^+$ [1]	
	3.2	$H_2CO \ldots OH^+$ [2] $+ H_2 + CH_3OH$ [2]	
	3.3	CH_3OH [2] $+ OH^+$ [2]	
	3.4	$CH_2(OH)_2 + H^+$ [2]	
	3.5	$HCOH$ [2] $+ H_2O$ [2] $+ H_2CO + H^+$ [2] $+ H_2$	22
4	4.1	CH_2OH^+ [1] $+ H_2O + CH_3OH$ [2]	
	4.2	$[CH_3O - - - -CH_2OH]^+ + H_2O$	
	4.3	$CH_3OCH_2OH + H_2O + H^+$ [(a)]	10, 12, 15, 18
5	5.1	$CH_2OH^+ + H_2O$	
	5.2	$HCO^+ + H_2 + H_2O$	
	5.3	$CO + H_2 + H_2O + H^+$ [(a)]	12, 18, 20

Notes. [1]Indicates the OH^+ projectile. [2]Indicate the second methanol molecules involved in the reactions, as well as the origin of their products. [(a)]Corresponds to a proton stabilized by hydrogen bonds with methanol molecules of the ice mantle in a $[H...OH...OH...OH]^+$ fashion.

20, and 22 eV, which is a representative range of energy where the richest chemistry happens along outflow regions.

A time step of 0.5 femtoseconds (fs) was chosen, to generate a total of 800 steps, allowing a timescale of 400 fs to analyze each trajectory after impact. The variables of energy and impact position were set up, using the ones selected previously (Inostroza-Pino et al. 2020, 2021; Inostroza et al. 2019). Throughout this series of articles, the projectile's charge is the only parameter that is modified. This variation allows us to compare what effect the charge-modification has on the COM formation pathways of $CH_2(OH)_2$ and CH_2OH, precursors of rich interstellar chemistry. All calculations were made using the Gaussian 09 code (Frisch et al. 2009).

3. Results and discussion

We analyze the chemical processes occurring after the impact through BOMD of $(CH_3OH)_{10}$ by OH^+, where methanediol $CH_2(OH)_2$ and the hydroxymethyl cation CH_2OH^+ were intermediates, to obtain stable complex organic molecules (COMs). In this section we discuss the formation of COMs such as methoxymethanol CH_3OCH_2OH, the formyl cation HCO^+, the Criegee biradical : $C(OH)_2$ (Samanta et al. 2014), and HCOH. We compare these findings on COMs with previous results obtained by Inostroza et al. (2019), Inostroza-Pino et al. (2020, 2021) where simulations kept the same conditions and the same target as the methanol cluster, with the projectiles OH^-, $OH^\bullet$, and OH^+. All the processes compared and discussed in this work have $CH_2(OH)_2$ and CH_2OH as intermediates. Both species are precursors of an interstellar molecule (Yocum et al. 2021; Silva et al. 2020) and also a relevant intermediate in the atmospheric ozonolysis reaction sequence (Zhu et al. 2022). In all cases, the reactants are $(CH_3OH)_{10} + OH^+$. These reactants generate the main outcomes listed in Table 1. To simplify the table, we have not included methanol molecules that are not part of the final products. It is important to note that all reactions fulfill the conservation of mass. For example, reaction 1 containing all reactants and products would be written $(CH_3OH)_{10} + OH^+ \longrightarrow CH_2(OH)_2 + H^+ + (CH_3OH)_9$.

3.1. *Methanediol* $CH_2(OH)_2$

This precursor has been described as one of the interstellar grain surface species (Gerakines et al. 1996; Yocum et al. 2021), even though it has not been detected yet in the ISM. It was recently synthesized in the laboratory for the first time via energetic processing of low-temperature methanol-oxygen ices (Zhu et al. 2022). In the same contribution, the authors performed calculations to explain how $CH_2(OH)_2$ is formed through the insertion of electronically excited atomic oxygen into a carbon-hydrogen bond of the methyl group of methanol followed by its stabilization in the icy matrix (Zhu et al. 2022).

Furthermore, Yocum et al. (2021) were able to detect and quantify a variety of COMs after ultraviolet photolysis of an ice sample of methanol CH_3OH. The authors identified the COMs as $CH_2OH^\bullet$, $CH_3O^\bullet$, and CH_3OCH_3 by sub-millimeter/far-IR spectroscopy and mass spectroscopy. However, a large number of signals remain unassigned since features may have more than one possible outcome within the mass charge range $m/z = 1-65$. This situation is a widespread problem in the laboratory and can be overcome with the help of simulations (Inostroza-Pino et al. 2014, 2009; Inostroza et al. 2013). In this context, simulations of a methanol ice mantle carried out by our group (Inostroza et al. 2019) have provided theoretical evidence of these possible formation pathways, structural geometries, and information about the isomers and reactive species related to the COMs mentioned above. This information may help distinguish these features, as the authors state.

We note which other COMs can be formed using $CH_2(OH)_2$ as a precursor. Table 1 shows the main outcomes observed after simulations. Reaction 1 identified methanediol $CH_2(OH)_2$ as a stable outcome. The process goes through the elimination of a proton via a nucleophilic substitution SN_2 mechanism at kinetic energies of 10, 15, and 18 eV. At higher impact energies (20–22 eV), $CH_2(OH)_2$ performs a secondary process (see reaction 2) that leads to COMs. The molecule $CH_2(OH)_2$ is the precursor of dihydroxymethylidene $:C(OH)_2$, also known as dihydroxycarbene (or Criegee), which is related to a series of unstable reactive carbene species (Jones et al. 2004). This type of species plays an important role in the oxidation of

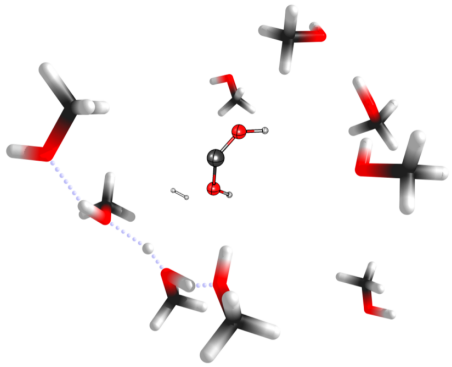

Fig. 1. Diagram illustrating reaction 2 yielding :$C(OH)_2 + H_2 + H^+$ transient hydrogen bonds stabilized by two or more methanol molecules in a BOMD simulation at 20 eV.

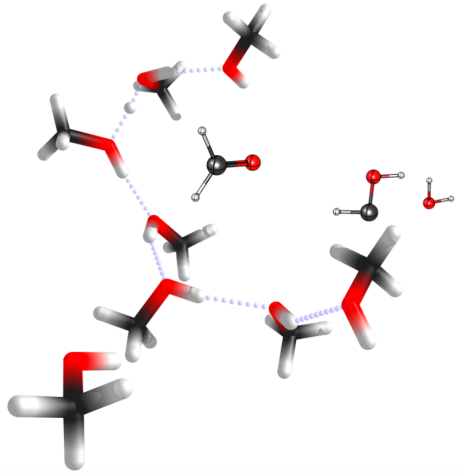

Fig. 2. Diagram illustrating reaction 3 yielding $H_2CO + HCOH + H^+ + H_2O$ outcomes at 22 eV, including the hydrogen bonds stabilized by two or more methanol molecules in a BOMD simulation.

unsaturated hydrocarbons with ozone (Quanz et al. 2020). It has been produced via thermal decomposition of oxalic acid in the gas phase (Schreiner & Reisenauer 2008). Dihydroxycarbene is the unstable tautomeric form of formic acid, which is the simplest organic carboxylic acid and precursor of a significant number of species in atmospheric chemistry (Hassan et al. 2021). Theoretical works (Zhu et al. 2022) support the laboratory findings, whereas diol and Criegee as intermediates are intrinsically involved in the environmental process. A recent review discussed the relevance of these key intermediates (Hassan et al. 2021). Reaction 2 in Table 1 describes the mechanism between the intermediates. The Criegee species is a stable product after diol formation pathways. Our BOMD simulations revealed the formation of dihydroxycarbene in conjunction with H_2 as products of the decomposition of methylene glycol $CH_2(OH)_2$. Figure 1 shows these findings. Our simulation results provide evidence for such a mechanism, although these alternative pathways can also be investigated in the laboratory.

In the process observed in reaction 3, the OH^+ impacts a methanol molecule to eliminate a dihydrogen molecule to produce $H_2CO + H_2 + OH^+$. The very reactive OH^+ is also generated due to the high energy involved in the process (22 eV). This second OH^+ impacts a second methanol molecule forming an unstable $CH_2(OH)_2 + H^+$. In the last step, the stabilization is a result of diol fragmentation producing H_2O and HCOH in a chair-like structure (Eq. (3.2), Table 1, reaction 3, and Fig. 2) at impact energies of 22 eV. We explained the potential energy surface (PES) using OH^+ to generate $CH_2(OH)_2$ followed by the H_2CO formation process at 22 eV. We also analyzed 14 ways to yield H_2CO starting from $(CH_3OH)_{10} + OH^+$ (Inostroza-Pino et al. 2021).

A similar process was observed by $OH^\bullet$ impacts (Inostroza-Pino et al. 2020). The results showed the key steps leading to $CH_2(OH)_2$. Depending on the kinetic impact energies and the impact positions, the diol $CH_2(OH)_2$ can be the final product (see reaction 3 on Table 1 of Inostroza-Pino et al. 2020). Diol can also undergo secondary and tertiary processes to generate stable outcomes as H_2CO and CH_3OCH_2OH. Table 1 in Inostroza-Pino et al. (2020) shows the processes to obtain mostly H_2CO in reactions 8, 9, and 12. Reaction 7 shows the formation of $HCO + H_2O + H_2$ and reaction 14 shows the pathway to form CH_3OCH_2OH.

3.2. *Hydroxymethyl cation* CH_2OH^+

Hydroxymethyl CH_2OH is the most favorable thermodynamic product of the reaction of $CH_3OH + OH^\bullet$ and it is found to be the dominant isomer at higher temperatures ($T > 400$ K) (Jasper et al. 2007; Nguyen et al. 2019). Even so, its detection in the interstellar medium has not been achieved. A plausible explanation is that this species is a highly reactive intermediate, playing a key role in forming other complex organic molecules (Gerakines et al. 1996). Later on Inostroza-Pino et al. (2020) found that CH_2OH is formed by the reaction of $(CH_3OH)_{10}$ either with $OH^\bullet$ or OH^+ at energies above 12 eV (Inostroza-Pino et al. 2020, 2021). In both cases, CH_2OH was an intermediate in the formaldehyde formation pathways, among other relevant COMs. This precursor underwent secondary or tertiary processes that lead to stable COMs such as formaldehyde H_2CO (Inostroza-Pino et al. 2021). We showed that chemistry using OH^+ and $OH^\bullet$ is richer than OH^-, even though the H_2Co was obtained as a stable outcome using $OH^-, OH^\bullet$, and OH^+ (Inostroza et al. 2019; Inostroza-Pino et al. 2020, 2021). Further investigations (Inostroza-Pino et al. 2021) pointed toward the necessary steps to produce the CH_2OH^+ intermediate from a reactive protonated methanediol. The latest intermediate underwent a dehydration reaction to yield a CH_2OH^+ intermediate, which eliminated a proton to form formaldehyde:

$$(CH_3OH)_{10} + OH^+ \longrightarrow CH_2(OH)_2 \ldots H^+, \quad (1)$$

$$CH_2OH^+ + H_2O \longrightarrow H_2CO + H_2O + H^{+a}. \quad (2)$$

The current work also shows that CH_2OH^+ is an intermediate in the formation routes of COMs such as methoxymethanol CH_3OCH_2OH (Schneider et al. 2019). The formation pathway of methoxymethanol has been proposed as the recombination of the methoxy and hydroxymethyl radicals (McGuire et al. 2017). Previously, we investigated this process using $OH^\bullet$ (Inostroza-Pino et al. 2020). We provide highlights of the mechanistic aspects involving those radicals and the non-detection of CH_2OH. In the same context, an experimental work proposed a new formation pathway using the CO-Hydrogenation process (He et al. 2022). They analyzed its formation by co-deposition of CO and H_2CO with H atoms, expecting that the recombination of the CH_2OH and CH_3O radicals occurs. However, as the authors claimed, the efficiency of these pathways was not sufficient to explain the observed abundance of methoxymethanol with respect to methanol. Unfortunately, the authors could not confirm the methoxymethanol formation in

this way. Moreover, methoxymethanol could not be detected at submillimeter wavelengths in the photo experiments of UV-photolyzed methanol ices because its detection limit is relatively high (Yocum et al. 2021). We investigated this pathway further, starting with the methanol ice mantle being hit by OH^+. The first step in reaction 4 is the proton abstraction to form H_2O and hydroxymethyl cation CH_2OH^+ at the range of kinetic impact energies 10, 12, 15, 18 eV. From here, a second CH_3OH molecule interacts to form a kind of adduct between $[C\ldots O\ldots H\ldots]^+$, which can finally undergo a proton elimination to yield CH_3OCH_2OH as a stable molecule. In this context, our previous report using $OH^\bullet$ (Inostroza-Pino et al. 2020) discussed the central aspect of forming methoxymethanol as well. Reaction 14 of Inostroza-Pino et al. (2020) explains the mechanisms to get from diol to methoxymethanol. Our results reveal step by step pathways that must be considered to explain the methoxymethanol abundances.

In reaction 5, once the OH^+ impacts a $(CH_3OH)_{10}$ ice mantle, a hydroxymethyl cation is formed, and a proton is released to form H_2O. The CH_2OH^+ produces its decomposition into a reactive formyl cation HCO^+, molecular hydrogen, and water (Eqs. (5.1) and (5.2)). The final step is the proton elimination from HCO^+ that leads to the formation of a carbonyl double bond C=O and the release of H^+ (Eq. (5.3)). When a proton is generated, it is stabilized by transient hydrogen bonds involving the nearest CH_3OH molecules.

These results are in agreement with previous theoretical evidence provided by Uggerud & Helgaker (1992) at the CASSCF level of theory, together with experimental evidence by Badin & Pacsu (1944). It reveals a concerted 1.2 elimination mechanism where one of the hydrogens originates from the carbon atom and the other from the oxygen atom. In addition, a similar process has been performed to obtain the formyl cation HCO^+ in the CH_3OH-rich ice experiment using UV irradiation (Öberg et al. 2009). The authors demonstrated that photolysis of CH_3OH-ices produces a recombination of the radicals, and the cation can generate new sublimated species, as we discovered in this work. In a previous contribution (Inostroza-Pino et al. 2021) we discussed that the formation of the formyl cation HCO^+ can lead to formaldehyde H_2CO (we refer to reaction 11 in that paper). We note that the highly reactive formyl cation interacts with CH_3OH, abstracting a hydride from its methyl group to produce formaldehyde. These pathways can explain why H_2CO is abundant in the ISM (Bacmann & Faure 2016).

Via simulations of OH^- (Inostroza et al. 2019), we described how those precursors yielded a secondary process to produce OCH_2OH^- (reaction 6), which has not been identified yet in the ISM. The HOCH in reaction 14 was also produced at impact energies of 18 and 20 eV. The formation mechanism for this molecule included both intermediates:

1) Diol formation: $CH_2(OH)_2 + H$;
2) Fragmentation: $CH_2(OH)_2 \longrightarrow CH_2OH^\bullet + H_2O + CH_3^\bullet$;
3) Proton abstraction: $CH_2OH^\bullet \longrightarrow HCOH + H_2O + CH_3OH$.

More recently, we showed that impacts on the $CH_3(OH)_{10}$ ice mantle by the $OH^\bullet$ radical yield the precursor $CH_2(OH)_2$ to produce $\cdot CH_2OH$, followed by the formation of $H_2CO + H_2O$ (see reactions 8, 9, and 12 of Inostroza-Pino et al. 2020). The methoxymethanol CH_3OCH_2OH was obtained after the CH_3O formation (see reaction 14 of Inostroza-Pino et al. 2020). We compared these results with the current simulations using OH^+. We kept the same structure of the $CH_3(OH)_{10}$ ice mantle, then selected the same kinetic impact energies ranges, and we used the same impact positions, where the only difference was the projectile charge. The comparison shows that the mechanisms go through different channels to yield the CH_3OCH_2OH product.

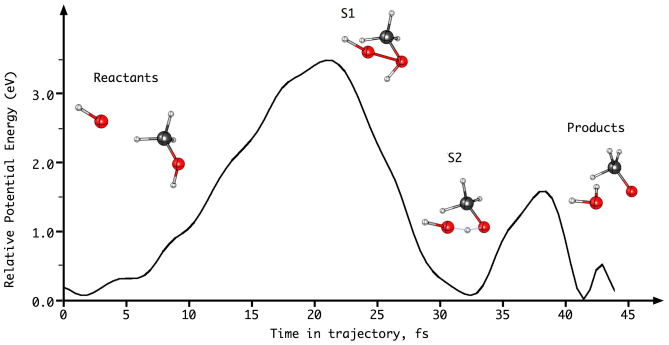

Fig. 3. Diagram illustrating $CH_3OH + OH^- \xrightarrow{CH_3OH--O--H} CH_3O^- + H_2O$ outcomes at 10 eV in a BOMD simulation.

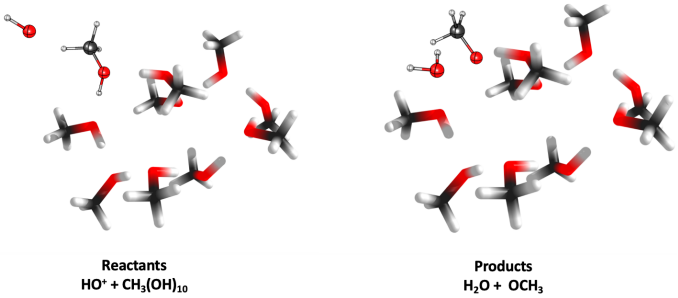

Fig. 4. Diagram illustrating (*a*) reactants and (*b*) products $CH_3OH + OH^- \longrightarrow CH_3O^- + H_2O$ outcomes at 10 eV in a BOMD simulation.

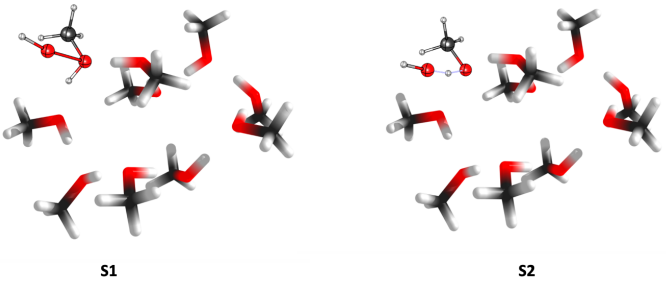

Fig. 5. Diagram illustrating (*c*) S1 $[CH_3 - (H - O - -O - H)^+]$ and (*d*) S2 $[CH_3O - H - -O - H]$ structures at 10 eV in a BOMD simulation.

Inostroza-Pino et al. (2020), also found that OCH_2OH was formed. Here reaction 5 at 10 eV produced $H_2 + {}^\bullet OCH_2OH$, to form H_2CO through a secondary process and their desorption from the mantle. In reaction 10 at 20 eV the $\cdot OCH_2OH$ radical is the main stable product.

Additionally, Inostroza et al. (2019) predicted that $CH_3O^- + H_2O$ was the most frequent outcome after impacts made by OH^-. This reaction was recently studied (Benitez et al. 2022) by photoelectron-photofragment coincidence spectroscopy (PPCS). The authors described the transition state structure and showed that $CH_3O{-}H_2O$ is a stable minimum. Our results are also in agreement with these laboratory results. It is important to note that we obtained the same intermediate throughout BOMD. The potential energy surface (PES) of the pathways mentioned above are depicted in Figs. 3–5. In our BOMD simulations the minimum is located with OH^- far from the $(CH_3OH)_{10}$. The energy increases to 3.3 eV when the projectile is closer to the $(CH_3OH)_{10}$; this intermediate structure is called S1 at

21.5 femtoseconds. Then the energy falls due to the proton interaction, forming a stable intermediate $[CH_3O - -H - -O - H]^*$ labeled S2 at 32.5 femtoseconds. The energy increases along with the bond arrangements. In the last step, due to the product stabilization of CH_3O^- + H_2O, at 40 femtoseconds, the energy decreases to form products (see the structural details of reactants S1-S2 and the products in Figs. 4 and 5). We could not observe these results using radical or cation projectiles, even when the only difference was the charge-projectile. The hydroxymethyl radical $CH_2OH^\bullet$ and methyleneglycol $CH_2(OH)_2$ were also observed in our BOMD within OH^- at higher kinetic impact energies (18 and 20 eV) to yield $CH_2O^\bullet, H_2CO$ together with its elusive HCOH isomer, as was discussed in Inostroza et al. (2019). In these BOMDs, it was possible to follow how the bond rearrangement is produced to obtain the primary intermediates followed by their corresponding final products.

These results can help experiments using PPCS techniques to detect the elusive CH_2OH^+ and $CH_2(OH)_2$ precursors in a reaction with $OH^\bullet$ radicals or OH^+ cations (Benitez et al. 2022).

4. Conclusion

We carried out simulations mimicking the formation and destruction processes of various molecular species through collisions with other atoms or molecules in the cloud and via ultraviolet photons to study formation pathways of astrochemical relevance species that have $CH_2(OH)_2$ and CH_2OH^+ in common, both of which are key organic precursors. Even though the intermediate compounds discussed in the current work have not yet been directly identified as a gaseous compound in the ISM, a remarkable experiment by Zhu et al. (2022) synthesized and identified the diol $CH_2(OH)_2$ for the first time by processing ices at low temperatures followed by gas-phase sublimation. These findings will allow the synthesis and characterization of unstable species (intermediates) in the Earth's atmosphere, and thus the prospective detection of these reactive intermediates using radio telescopes. In addition, our results indicate that these intermediate species $CH_2(OH)_2$ and CH_2OH^+ are part of reactions that lead to the formation of stable products such as formaldehyde H_2CO. Additionally, Geppert et al. (2006) also indicated that these two species lead to the main intermediate species in formaldehyde formation. Studies by Franco et al. (2021) proposed that the atmospheric formation of formaldehyde comes from the fast oxidation of methanediol $CH_2(OH)_2$, transforming it into a very important intermediate in the processes that occur in the Earth's atmosphere. In light of our results, whenever $CH_2(OH)_2$ or CH_2OH^+ intermediates were formed, they underwent secondary or tertiary processes to form stable products.

We show an alternative route to obtain methoxymethanol CH_3OCH_2OH, the formyl cation HCO^+, the Criegee $:C(OH)_2$ biradical, formaldehyde H_2CO, and HCOH in a chair-like structure, species which are released to the gas phase. Owing to our results, we can say with certainty that $CH_2(OH)_2$ acts in a primary process to lead to new COMs and is also a final product. In the case of identifying methanediol as the final product, this process involves the elimination of a proton through the SN_2 nucleophilic substitution mechanism at kinetic energies of 10, 15, and 18 eV where $CH_2(OH)_2$ and CH_2OH^+ intermediates undergo secondary and tertiary processes leading to stable products. Our results demonstrate that the bombardment of methanol ice mantles by OH^+ cations produces CH_3O and CH_2OH recombinations to form methoxymethanol if CH_2OH^+ is present (McGuire et al. 2017). In addition, $CH_2(OH)_2$ is the precursor to the Criegee intermediate $:C(OH)_2$, which is related to several reactive and unstable carbene species. It is essential to note that all projectiles OH^-, $OH^\bullet$, and OH^+ produced H_2CO as well. The formation of H_2CO is independent of the kinetic impact energy employed showing different formation mechanisms via different crucial precursors. The pathways in some cases go through $CH_2(OH)_2$ or go through CH_2OH^+. Due to the charge on projectiles, the difference seems irrelevant in the final product, though this aspect must be corroborated in laboratory experiments. As we show, different intermediates in a variety of mechanisms generate H_2CO, providing a good explanation for the high interstellar abundance of H_2CO. The mechanisms found here can give insight into alternative pathways relevant to understanding experimental processes with key steps within those intermediates. It is essential to note that the chemistry revealed throughout these contributions can explain different pathways and improve molecular assignments from methanol ices. Thus, mantles under impacts with OH^+can provide information into ion-ice reactions in protostellar envelopes where the ice chemistry is dominated by pure CH_3OH chemistry. Hence, similar outcomes to the one we give here should be expected in the gas-phase over a wide range of interstellar objects (Öberg et al. 2009; Dartois et al. 1999; Carrascosa et al. 2020).

Acknowledgements. The authors give thanks for the support of FONDECYT-Chile grant 11140770, PCI-ANID International Networks Grant REDES190113 and the European Union's Horizon 2020 research and innovation program under the Marie Skłodowska-Curie grant agreement No. 872081 (ATMOS). C.H. acknowledges support from DIUA 225-2021.

References

Bacmann, A., & Faure, A. 2016, A&A, 587, A130
Badin, E. J., & Pacsu, E. 1944, J. Am. Chem. Soc., 66, 1963
Barrientos, C., Redondo, P., Martínez, H., & Largo, A. 2014, ApJ, 784, 132
Benitez, Y., Nguyen, T. L., Parsons, A. J., Stanton, J. F., & Continetti, R. E. 2022, J. Phys. Chem. Lett., 13, 142
Bolton, K., Hase, W. L., & Peslherbe, G. H. 1998, Modern Methods for Multidimensional Dynamics Computations in Chemistry (Singapore: World Scientific), 143
Boogert, A. A., Gerakines, P. A., & Whittet, D. C. 2015, ARA&A, 53, 541
Borrás-Almenar, J., Clemente-Juan, J. M., Coronado, E., & Tsukerblat, B. S. 2001, MAGPACK 1 A package to calculate the energy levels, bulk magnetic properties, and inelastic neutron scattering spectra of high nuclearity spin clusters (Wiley Online Library)
Boyd, S. L., & Boyd, R. J. 2007, J. Chem. Theory Comput., 3, 54
Brown, W. A., & Bolina, A. S. 2007, MNRAS, 374, 1006
Burke, D., Puletti, F., Brown, W., et al. 2015, MNRAS, 447, 1444
Burkhardt, A. M., Shingledecker, C. N., Le Gal, R., et al. 2019, ApJ, 881, 32
Carrascosa, H., Cruz-Díaz, G. A., Muñoz Caro, G. M., Dartois, E., & Chen, Y. J. 2020, MNRAS, 493, 821
Check, C. E., Faust, T. O., Bailey, J. M., et al. 2001, J. Phys. Chem. A, 105, 8111
Chen, J., Ma, R., Ren, H., et al. 2005, Int. J. Mass Spectrom., 241, 25
Dartois, E., Schutte, W., Geballe, T., et al. 1999, A&A, 342, L32
Dupuy, R., Bertin, M., Féraud, G., et al. 2018, Nat. Astron., 2, 796
Franco, B., Blumenstock, T., Cho, C., et al. 2021, Nature, 593, 233
Fredon, A., & Cuppen, H. 2018, PCCP, 20, 5569
Fredon, A., Lamberts, T., & Cuppen, H. 2017, ApJ, 849, 125
Frisch, M. J., Trucks, G. W., Schlegel, H. B., et al. 2009, Gaussian09 Revision A.1 (Wallingford CT: Gaussian Inc.), 2009
Gadre, S. R., Yeole, S. D., & Sahu, N. 2014, Chem. Rev., 114, 12132
Garrod, R. 2008, A&A, 491, 239
Garrod, R. T., Wakelam, V., & Herbst, E. 2007, A&A, 467, 1103
Geppert, W. D., Hamberg, M., Thomas, R. D., et al. 2006, Faraday Discuss., 133, 177
Gerakines, P., Schutte, W., & Ehrenfreund, P. 1996, A&A, 312, 289
Gordon, M. 1982, J. Am. Chem. Soc., 104, 2797
Hama, T., & Watanabe, N. 2013, Chem. Rev., 113, 8783
Hassan, Z., Stahlberger, M., Rosenbaum, N., & Bräse, S. 2021, Angew. Chem. Int. Ed, 60, 15138
He, J., Simons, M., Fedoseev, G., et al. 2022, A&A, 659, A65
Helgaker, T., Uggerud, E., & Jensen, H. J. A. 1990, Chem. Phys. Lett, 173, 145
Inostroza, N., Fortenberry, R. C., Huang, X., & Lee, T. J. 2013, ApJ, 778, 160

Inostroza, N., Mardones, D., Cernicharo, J., et al. 2019, A&A, 629, A28
Inostroza-Pino, N., Letelier, R., & Senent, M. L. 2009, J. Math. Chem., 45, 1055
Inostroza-Pino, N., Cardenas, C., & Fuentealba, P. 2014, MNRAS, 443, 3127
Inostroza-Pino, N., Mardones, D., Ge, J. J. X., & MacLeod-Carey, D. 2020, A&A, 641, A14
Inostroza-Pino, N., MacLeod-Carey, D., Heyser, C., et al. 2021, A&A, 650, A169
Jasper, A. W., Klippenstein, S. J., Harding, L. B., & Ruscic, B. 2007, J. Phys. Chem. A., 111, 3932
Jones, M. J., & Moss, R. A. 2004, in Reactive Intermediate Chemistry, eds. R. A. Moss, M. S. Platz, & M. J. Jones (Hoboken, New Jersey: John Wiley & Sons, Inc.)
Kent, D. R., IV, Widicus, S. L., Blake, G. A., & Goddard, W. A., III 2003, J. Chem. Phys., 119, 5117
Maté, B., Cazaux, S., Satorre, M. Á., et al. 2020, A&A, 643, A163
McBride, E., Millar, T., & Kohanoff, J. 2013, J. Phys. Chem. A, 117, 9666
McGuire, B. A., Shingledecker, C. N., Willis, E. R., et al. 2017, ApJ, 851, L46
Miyazaki, A., Watanabe, N., Sameera, W., et al. 2020, Phys. Rev. A, 102, 052822
Nguyen, T. L., Ruscic, B., & Stanton, J. F. 2019, J. Chem. Phys, 150, 084105
Oberg, K. I. 2016, Chem. Rev., 116, 9631
Öberg, K. I., Garrod, R. T., van Dishoeck, E. F., & Linnartz, H. 2009, A&A, 504, 891
Öberg, K. I., Boogert, A. A., Pontoppidan, K. M., et al. 2011, ApJ, 740, 109
Pantaleone, S., Enrique-Romero, J., Ceccarelli, C., et al. 2020, ApJ, 897, 56
Pantaleone, S., Enrique-Romero, J., Ceccarelli, C., et al. 2021, ApJ, 917, 49
Pires, M. M., & DeTuri, V. F. 2007, J. Chem. Theory Comput., 3, 1073
Quanz, H., Bernhardt, B., Erb, F. R., et al. 2020, J. Am. Chem. Soc., 142, 19457
Samanta, K., Beames, J. M., Lester, M. I., & Subotnik, J. E. 2014, J. Chem. Phys., 141, 134303
Schreiner, P. R., & Reisenauer, H. P. 2008, Angew. Chem. Int. Ed., 47, 7071
Schneider, H., Caldwell-Overdier, A., Coppieterst Wallant, S., et al. 2019, MNRAS, 485, L19
Shingledecker, C. N., Vasyunin, A., Herbst, E., & Caselli, P. 2019, ApJ, 876, 140
Silva, S. G., Vichietti, R. M., Haiduke, R. L., Machado, F. B., & Spada, R. F. 2020, MNRAS, 497, 4486
Taban, I., Schutte, W., Pontoppidan, K., & Van Dishoeck, E. 2003, A&A, 399, 169
Tielens, A., & Hagen, W. 1982, A&A, 114, 245
Tsuge, M., & Watanabe, N. 2021, Acc. Chem. Res., 54, 471
Uggerud, E., & Helgaker, T. 1992, J. Am. Chem. Soc., 114, 4265
Van de Sande, M., Walsh, C., Mangan, T. P., & Decin, L. 2019, MNRAS, 490, 2023
Yocum, K., Milam, S., Gerakines, P., & Weaver, S. W. 2021, ApJ, 913, 61
Zhu, C., Kleimeier, N. F., Turner, A. M., et al. 2022, PNAS, 119